



SPring-8/SACLA Research Frontiers 2019

CONTENTS

Preface	5
Editor's Note	6
Scientific Frontiers	7
Review	
Synchrotron radiation-based X-ray analysis for cultural heritage and art <i>Y. Abe</i>	8
Life Science	
 Serial femtosecond crystallography: Oxyl/oxo coupling mechanism for dioxygen formation in photosystem II <i>M. Suga and J.-R. Shen</i>	12
High-resolution protein crystallography: Charge-density analysis of green fluorescent protein at ultra-high resolution <i>K. Takaba and K. Takeda</i>	14
Protein crystallography: Crystal structure of heliorhodopsin <i>W. Shihoya</i>	16
Protein crystallography: Discovery of cap-specific adenosine- N^6 -methyltransferase (CAPAM) <i>S. Akichika, S. Hirano, O. Nureki and T. Suzuki</i>	18
Protein crystallography: <i>In crystallo</i> thermodynamic analysis of catalytic reaction in bacterial copper amine oxidase <i>T. Murakawa, S. Baba and T. Okajima</i>	20
Protein crystallography: Mechanism of stress-induced inhibition of eukaryotic translation initiation factor 2B <i>K. Kashiwagi and T. Ito</i>	22
Protein hydration: Sugars can protect hydration shell of proteins and stabilize their native structures in crowded molecular environment: clarified by complementary use of X-rays and neutrons <i>M. Hirai</i>	24
Neurology: Parkinson's disease is a type of amyloidosis characterized by accumulation of amyloid fibrils of α -synuclein <i>K. Araki, N. Yagi and H. Mochizuki</i>	26
Ophthalmology: Gradient of index and moduli is essential for optimal function of the eye lens <i>K. Wang, M. Hoshino and B. K. Pierscionek</i>	28

Physical Science

- Nuclear clock:** Active pumping of ^{229}Th nuclear clock isomer by synchrotron radiation-based nuclear resonant scattering 30
T. Masuda, T. Hiraki, A. Yoshimi and K. Yoshimura
- Barocaloric effect:** Pressure-induced phase transition in plastic crystal neopentylglycol with colossal barocaloric effects 32
B. Li, T. Sugahara and K. Li
- Martensitic transformation:** Discovery of simple variant selection effect during stress-driven martensitic transformation 34
B. Yue, F. Hong and B. Chen
-  **Ultrafast dislocation behavior:** Studying ultrafast dynamics of temperature-dependent dislocation in Fe-0.1mass% C using femtosecond X-ray diffraction 36
M. Yonemura
- Spin dynamics:** Direct evidence of Co-3d orbital change associated with spin crossover in LaCoO_3 obtained by X-ray Compton scattering 38
Y. Kobayashi
- Solid oxygen:** Oxygen K-edge X-ray Raman spectroscopy for solid oxygen up to 140 GPa with hard X-rays 40
H. Fukui
- Magnetic anisotropy:** The magnetic anisotropy of graphene-covered cobalt on silicon carbide 42
R. Hönig, T. Ohkochi and C. Westphal
- Antiferromagnetic domain motion:** Magnetoelectric-effect-driven antiferromagnetic domain motion revealed by scanning soft X-ray magnetic circular dichroism microscopy 44
Y. Shiratsuchi
- Inelastic scattering:** Signature of rigidity transition in liquid As_2Se_3 observed by inelastic X-ray scattering 46
M. Inui, A. Q. R. Baron and Y. Kajihara
-  **Superfluorescence:** First observation of ‘superfluorescence’ at extreme ultra-violet wavelengths 48
J. R. Harries, H. Iwayama and S. Kuma

Chemical Science

- Photoactuator molecule:** Object transport system mimicking the cilia of *Paramecium Aurelia*, making use of the light-controllable crystal bending behavior of photochromic diarylethene 50
K. Uchida, R. Nishimura and A. Fujimoto
- Multifunctional liquid crystal:** Supramolecular polymerization in liquid crystalline media enables modular approach to multifunctional core-shell columnar coassembly 52
K. Yano, Y. Itoh and T. Aida
- Crystal-like droplet:** Single-crystal-like chiral organic droplets exhibiting unidirectional rotating sliding 54
T. Kajitani

	Diamond semiconductor: Determination of the 3D local structures of dopant in heavily phosphorus-doped diamond <i>T. Yokoya, H. Kato and T. Matsushita</i>	56
	Ultrafast X-ray spectroscopy: Tracking multiple components of a nuclear wavepacket in photexcited Cu(I)-phenanthroline complex using ultrafast X-ray spectroscopy <i>T. Katayama</i>	58
	Hydrogen bonds: Environmental effects on the nature of hydrogen bonding detected by synchrotron FTIR microspectroscopy <i>M. Takahashi</i>	60
	Catalytic converter: Dynamic behavior of Rh species in Rh/Al ₂ O ₃ model catalyst during three-way catalytic reaction: An <i>operando</i> X-ray absorption spectroscopy study <i>H. Asakura, S. Hosokawa, K. Teramura and T. Tanaka</i>	62
	Fuel cells: <i>Operando</i> observation of sulfur species that poison polymer electrolyte fuel cell studied by near ambient pressure hard X-ray photoelectron spectroscopy <i>T. Yokoyama and Y. Iwasawa</i>	64
	Fuel cells: <i>Operando</i> three-dimensional imaging of distribution and degradation process of Pt-Co cathode catalyst in polymer electrolyte fuel cell <i>H. Matsui, Y. Tan and M. Tada</i>	66
	PEFC catalyst: Electrical double layer structure that activates the oxygen reduction reaction <i>T. Kumeda, O. Sakata and M. Nakamura</i>	68
	Spectro-ptychography: Oxygen-diffusion-driven oxidation behavior and tracking areas visualized by X-ray spectro-ptychography with unsupervised learning <i>Y. Takahashi, H. C. Dam and M. Tada</i>	70
	Soil science: Speciation of phosphorus and zinc in soils receiving swine manure compost for nearly a quarter of a century <i>Y. Hashimoto, K. Yamamoto and J. Kang</i>	72
 Earth & Planetary Science		
	Mantle dynamics: Sharp 660-km seismic discontinuity explained by extremely narrow binary post-spinel transition <i>T. Ishii and T. Katsura</i>	74
	Mantle dynamics: Laboratory measurements of sound velocities of CaSiO ₃ perovskite reveal the fate of subducted oceanic crust into the Earth's deep interior <i>S. Gréaux and T. Irifune</i>	76
	Core dynamics: Earth's cooler core inferred from new resistance-heated diamond-anvil-cell experiments <i>R. Sinmyo, K. Hirose and Y. Ohishi</i>	78
	Planetary science: Imaging fossil asteroidal ice in primitive meteorite by synchrotron radiation-based X-ray computed nanotomography <i>M. Matsumoto</i>	80

Industrial Applications

Piezoelectric device: Investigation of crystallographic deformation by converse piezoelectric effect of piezoelectric thin films <i>G. Tan and I. Kanno</i>	82
Metal/polymer interface: Revealing interfacial chemistry between metal and polymer by hard X-ray photoelectron spectroscopy <i>Y. Kubo</i>	84

Accelerators & Beamlines Frontiers 86

SPring-8

Beam Performance	87
-------------------------	----

New Apparatus, Upgrades & Methodology

<ul style="list-style-type: none"> • New highly efficient and fully automatic MX at SPring-8 BL45XU beamline <i>S. Baba, K. Hirata, N. Mizuno and T. Kumasaka</i> 	88
--	----

SACLA

Beam Performance	91
-------------------------	----

New Apparatus, Upgrades & Methodology

<ul style="list-style-type: none"> • Generation of high-intensity narrowband X-ray Free Electron Laser through reflection self-seeding <i>I. Inoue, T. Osaka and M. Yabashi</i> 	92
--	----

Facility Frontiers 94

SPring-8 Facility Status	95
Introduction	95
Machine Operation	96
Beamlines	97
User Program and Statistics	100
Research Outcome	103
Budget and Personnel	103
Research Complex	103
SPring-8 Users Community (SPRUC)	105
Outreach Activities	106
SACLA Facility Status	107

Note: The principal publication(s) concerning each article is indicated with all author's names in italics in the list of references.